EUROPHYSICS LETTERS 15 November 2001

Europhys. Lett., **56** (4), pp. 563–569 (2001)

Phase diagram of the Hubbard model: Beyond the dynamical mean field

M. Jarrell[1], Th. Maier[2], M. H. Hettler[3] and A. N. Tahvildarzadeh[1]

[1] *Department of Physics, University of Cincinnati - Cincinnati, OH 45221, USA*
[2] *Institut für Theoretische Physik, Universität Regensburg*
93040 Regensburg, Germany
[3] *Forschungszentrum Karlsruhe - Postfach 3640, 76021 Karlsruhe, Germany*

(received 27 March 2001; accepted in final form 30 August 2001)

PACS. 71.10.-w – Theories and models of many-electron systems.
PACS. 71.10.Hf – Non-Fermi liquid ground states, electron phase diagrams and phase transitions in model systems.
PACS. 74.20.-z – Theories and models of superconducting state.

Abstract. – The Dynamical Cluster Approximation (DCA) is used to study non-local corrections to the dynamical mean-field phase diagram of the two-dimensional Hubbard model. Regions of antiferromagnetic, *d*-wave superconducting, pseudo-gapped non-Fermi liquid, and Fermi liquid behaviors are found, in rough agreement with the generic phase diagram of the cuprates. The non-local fluctuations beyond the mean field both suppress the antiferromagnetism and mediate the superconductivity.

Introduction. – The rich phenomenology of high-T_c superconductors [1] has stimulated strong experimental and theoretical interest in the field of strongly correlated electron systems. Common to all high-T_c systems is the presence of antiferromagnetic ordering in undoped samples in proximity to a superconducting phase with a *d*-wave order parameter and the normal state pseudogap dominating the physics in underdoped samples. A successful theory must describe all these fundamental features at the same time.

The 2D Hubbard model in the intermediate coupling regime or closely related models like the t-J model are believed to capture the essential physics of the high-T_c cuprates [2]. The antiferromagnetic phase of the cuprates is well understood. In the strong-coupling limit $U \gg W$, where U is the Coulomb repulsion and W the bare bandwidth, the undoped Hubbard model reduces to the Heisenberg model, which has been proven to describe the low-energy spin fluctuations of the cuprate parent compounds. However, off half-filling there is no complete understanding of the superconducting phase or the normal-state pseudogap in the intermediate-coupling 2D Hubbard model.

Finite-size quantum Monte Carlo (QMC) calculations for the doped 2D Hubbard model in the intermediate coupling regime with $U \sim W$ support the idea of a spin fluctuation driven interaction mediating *d*-wave superconductivity [3]. However, the fermion sign problem and the fact that the number of degrees of freedom grows rapidly with the lattice size limit these

calculations to temperatures too high to study a possible transition [3]. These calculations are also restricted to relatively small system sizes, making statements for the thermodynamic limit problematic, and inhibiting studies of the low-energy physics.

These shortcomings do not apply to the Dynamical Mean Field Approximation (DMFA), which is by construction in the thermodynamic limit. Unfortunately, the lack of non-local dynamics in the DMFA inhibits a possible transition to a state with a non-local (d-wave) order parameter.

However, it is well known within phenomenological theories that short-ranged antiferromagnetic spin fluctuations mediate pairing with d-wave symmetry and cause a pseudogap in underdoped samples [3–5]. There is experimental evidence that the correlation length of dynamical spin fluctuations in the optimally doped cuprates is very small [6]. Therefore, microscopic studies, which account for short-ranged dynamical correlations in addition to the local correlations of the DMFA, are relevant and might succeed in describing the physics of the cuprates.

The recently developed Dynamical Cluster Approximation (DCA) [7–9] is a fully causal approach which systematically incorporates these non-local corrections to the DMFA by mapping the lattice problem onto an embedded periodic cluster of size N_c. For $N_c = 1$ the DCA is equivalent to the DMFA and by increasing N_c the dynamic correlation length can be gradually increased while the calculation remains in the thermodynamic limit. Previous DCA calculations have indicated the presence of an extended d-wave superconducting phase at moderate doping [8–10].

In this manuscript we present calculations of the full phase diagram of the 2D Hubbard model studied with the DCA. To solve the cluster problem we use QMC. We choose $N_c = 4$, the smallest cluster that includes non-local corrections while preserving the full translational and point group symmetries of the lattice. The results are compared to DMFA calculations, $N_c = 1$, to illustrate the effect of the initial non-local corrections.

Formalism. – A detailed discussion of the DCA formalism was given in previous publications [7–9, 11]. The compact part of the free energy is coarse-grained in reciprocal space, projecting it onto a finite-sized cluster of N_c points embedded in a self-consistently determined host. The cluster problem is solved using the Hirsch-Fye impurity algorithm [12] modified to simulate an embedded cluster [11], and the spectra are analytically continued with the maximum entropy method [13]. Once the cluster problem has been solved, lattice susceptibilities may be calculated [7]. All calculations are done in the normal, paramagnetic state. We search for continuous phase transitions indicated by the divergence of the corresponding susceptibilities.

The Hubbard model is characterized by a near-neighbor hopping t and a one-site repulsion U. We choose $t = 1/4$ to establish a unit of energy and choose $U = W = 2$ which is sufficiently large that for $N_c \geq 4$, a Mott gap is present in the half-filled model. The phase diagram of the Hubbard model, calculated with DMFA, displays a range of behaviors including Mott insulating, antiferromagnetic and Fermi-liquid regimes [14]. The inclusion of non-local corrections yields significant changes to the phase diagram, including the enhancement of the Mott phase at half-filling [15], the suppression of antiferromagnetism, the introduction of a d-wave superconducting phase and non-Fermi-liquid behavior. These different regimes are delineated by calculating the antiferromagnetic (fig. 1), bulk magnetic (fig. 2) and d-wave superconducting (fig. 4) susceptibilities, and the single-particle self-energy (fig. 3).

Antiferromagnetism. – In fig. 1, the inverse antiferromagnetic susceptibility is plotted *vs.* temperature for dopings $\delta = 0$ and 0.05 and $N_c = 4$ and 1. We plot the inverse susceptibility to show that, in contrast to finite-sized system calculations, the susceptibility diverges for

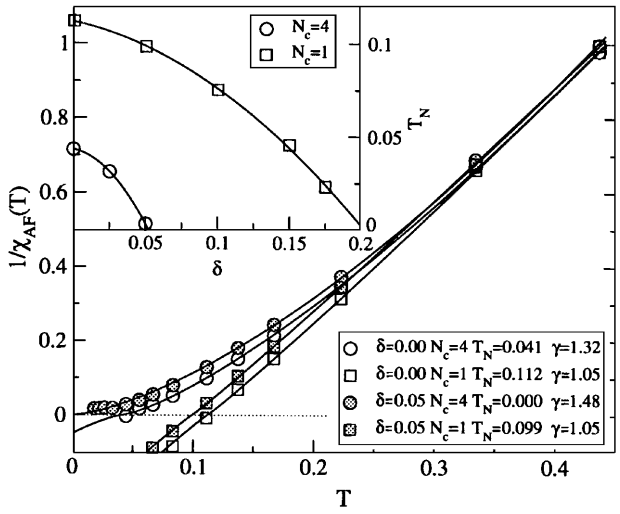

Fig. 1 – Inverse antiferromagnetic susceptibility *vs.* temperature for $U = 2$. The lines are fits to the function $1/\chi_{\mathrm{AF}}(T) = b(T - T_N)^{\gamma}$. For $N_{\mathrm{c}} = 1$, $\gamma \approx 1$, the mean-field value. For $N_{\mathrm{c}} = 4$ non-local fluctuations suppress the transition, so that γ increases and T_N decreases (see inset).

low doping at $T = T_N$. This indicates a transition to an antiferromagnetic phase. In the DMFA for the 2D model, or as we found previously for the infinite-dimensional model [14], the antiferromagnetism persists to relatively high temperatures and dopings. The non-local dynamical fluctuations, included in the DCA for $N_{\mathrm{c}} > 1$, strongly suppress the antiferromagnetism. Their effect becomes pronounced for low temperatures and dopings. For example, when $\delta = 0$, the $N_{\mathrm{c}} = 1$ and $N_{\mathrm{c}} = 4$ AF susceptibilities are identical at high temperatures due to the lack of non-local correlations, but separate as the temperature is lowered. The $N_{\mathrm{c}} = 1$ susceptibility diverges with mean-field exponent of about one whereas the $N_{\mathrm{c}} = 4$ result diverges at a much lower temperature with a larger exponent. Consistent with the Mermin Wagner theorem, T_N continues to fall for large values of N_{c} (not shown).

The pseudogap and non-Fermi-liquid behavior. – The bulk ($\boldsymbol{k} = 0$) magnetic susceptibility and single-particle density of states (DOS) display evidence of a pseudogap for low doping $\delta < 0.2$. We show the bulk magnetic susceptibility in the inset to fig. 2 for three different dopings. For low to intermediate doping, it develops a peak at low temperatures, defining a temperature T^*. $T^* \sim T_N(N_{\mathrm{c}} = 1)$, the mean-field transition temperature (see figs. 5 and 1). For $N_{\mathrm{c}} > 1$, it defines the temperature where short-ranged spin correlations first emerge. The underdoped bulk susceptibility data, $\delta \sim 0.075$, may be scaled onto one curve by plotting *vs.* T/T^* (not shown). A similar peak or downturn and scaling is seen in the Knight-shift data of the cuprates [1]. The downturn of the susceptibility is accompanied by a loss of states near the Fermi energy. For temperatures $T < T^*$, a pseudogap begins to develop in the DOS, as shown in fig. 2. The pseudogap is widest, measured from peak to peak, at low doping, and vanishes for $\delta \gtrsim 0.2$. The depth of the pseudogap is greatest when $\delta \approx 0.05$, and it vanishes as $\delta \to 0$, where it is replaced by a Mott gap of width $\approx U$.

The slow fall of T^* with doping indicates that the short-ranged spin correlations diminish slowly upon doping. Thus, even in the region $T^* > T > T_N$ the antiferromagnetic correlations still have a significant effect. This is supported by the behavior of the self-energy for temperatures $T < T^*$. Once the DCA algorithm is converged, the lattice self-energy is calculated

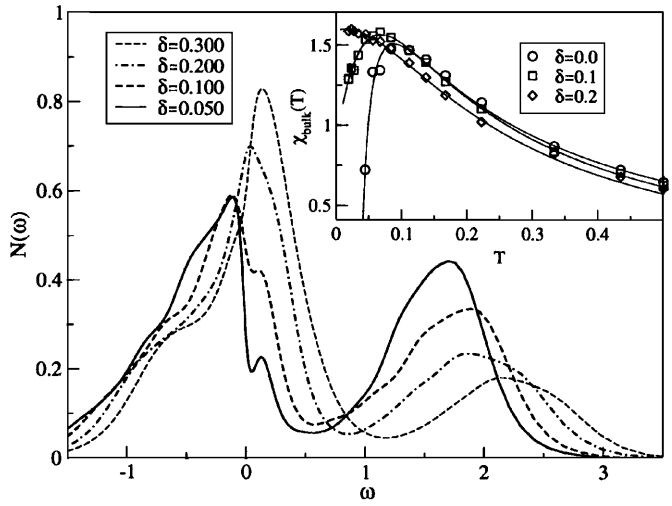

Fig. 2 – The single-particle density of states $N(\omega)$ for $U = 2$, $T = 0.023$ and $N_c = 4$. The inset shows the bulk susceptibility as a function of temperature. For $\delta < 0.2$ a peak develops at $T = T^*$ accompanied by the evolution of a pseudogap in the DOS for $T < T^*$.

by interpolating the cluster result on to the full lattice Brillouin zone. Thus the lattice self-energy at any $\boldsymbol{k}$ is dominated by the cluster self-energy at the nearest cluster momentum. For a Fermi liquid, the self-energy $\Sigma(\boldsymbol{k}, \omega) \sim (1 - 1/Z)\omega - ib\omega^2$, where $b > 0$ and $1/Z > 1$. Our results show that, near half-filling, the self-energy displays non-Fermi-liquid behavior. This is illustrated in fig. 3, where we plot the low-frequency self-energy at the DCA cluster momenta for $\delta = 0.05$ and $T = 0.023$. For momentum points near $\boldsymbol{k} = (\pi, 0)$, the imaginary part of the self-energy crosses the Fermi energy almost linearly. Concomitant with this behavior is a pseudogap of width $\approx |J| \approx 4t^2/U$ in the single-particle spectra $A(\boldsymbol{k}, \omega)$ for momenta near $\boldsymbol{k} = (\pi, 0)$ (not shown).

The pseudogap and the anomalies in the self-energy vanish when T^* falls to zero. Here,

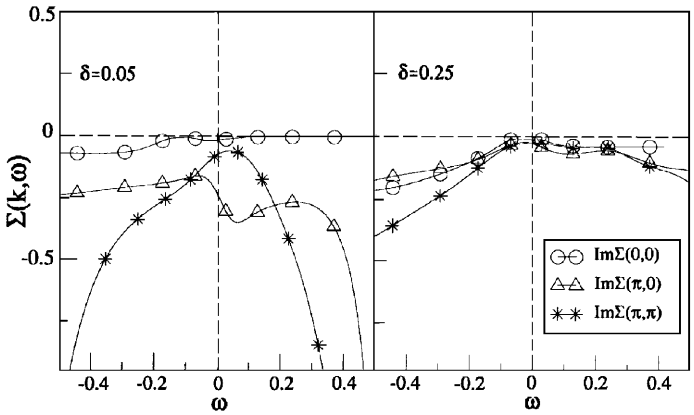

Fig. 3 – The imaginary part of the single-particle self-energies at the DCA cluster momenta, plotted *vs.* frequency ω for $U = 2$, $T = 0.023$, $N_c = 4$ and $\delta = 0.05$ (left) and $\delta = 0.25$ (right). The self-energy at $(\pi, 0)$ changes from non-Fermi-liquid–like at doping $\delta = 0.05$ to Fermi-liquid–like at $\delta = 0.25$. The dashed lines indicate the zero axes.

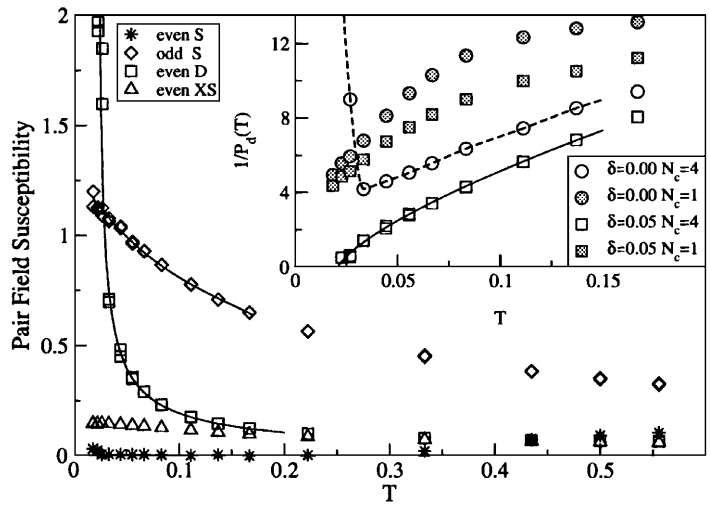

Fig. 4 – The s-wave, extended s-wave, and d-wave even-frequency and the odd-frequency s-wave $\boldsymbol{q} = 0$ susceptibilities *vs.* temperature for $U = 2.0$, $\delta = 0.05$, and $N_c = 4$. Pairing is found only in the even-frequency $\boldsymbol{q} = 0$ d-wave channel. In the inset the inverse d-wave pair-field susceptibility is plotted *vs.* temperature for two different dopings and cluster sizes. The line is a fit to $1/P_d(T) = b(T - T_c)^\gamma$ with $T_c = 0.021$ and $\gamma = 0.72$.

as shown on the right of fig. 3, the self-energy becomes Fermi-liquid–like with quasiparticle weight $Z \approx 1/2$. A systematic study of the evolution of the single-particle spectra and the Fermi surface will be presented elsewhere.

It is important to stress that the pseudogap, the downturn of the bulk magnetic susceptibility and the non-Fermi-liquid behavior in the self-energy are *absent* when $N_c = 1$ due to the lack of non-local fluctuations.

Superconductivity. – We searched for many different types of superconductivity, including s, extended-s, p and d waves, of both odd and even frequency and we looked for pairing at both the zone center and corner. Of these, only the odd-frequency s-wave and even-frequency d-wave pair-field susceptibilities at the zone center were strongly enhanced, and only the d-wave susceptibility diverged. This is illustrated in fig. 4 where the odd-frequency s-wave and the even-frequency d-wave $\boldsymbol{q} = 0$ susceptibilities are plotted *vs.* temperature for $U = 2$ and $\delta = 0.05$. The s-wave and extended s-wave $\boldsymbol{q} = 0$ even-frequency susceptibilities are also plotted for comparison.

The behavior of the d-wave pair-field susceptibility as a function of temperature for $N_c = 1$ and 4 and $\delta = 0$ and 0.05 is shown in the inset to fig. 4. For $N_c = 1$ there is no tendency towards pairing. For the DMFA there is no pairing with symmetries lower than the lattice symmetry (*i.e.*, p-, d-wave, etc.) [16].

d-wave pairing is strongly enhanced for $N_c = 4$ over the corresponding DMFA results. However, for $\delta = 0$ the inverse susceptibility rises abruptly as the temperature is lowered and the Mott gap opens in the DOS. The Mott gap becomes more pronounced as N_c increases [15], so that for larger clusters the gap prevents superconductivity even for $U < W$. If charge excitations are gapped, then pairing is suppressed. At half-filling, for $U = 2$ the gap is of order U, and is much larger than the magnetic exchange energy $|J| \sim 4t^2/U = 0.125$, so that the opening of the Mott gap will suppress any magnetically mediated pairing. Away from half-filling the width of the pseudogap in the charge excitation spectrum is much smaller, on

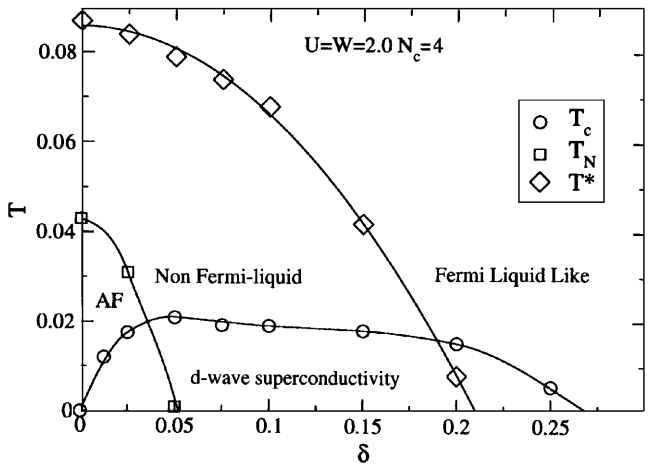

Fig. 5 – The temperature-doping phase diagram of the 2D Hubbard model calculated with QMC and DCA for $N_c = 4$, $U = 2$. T_N and T_c were calculated from the divergences of the antiferromagnetic and d-wave susceptibilities, respectively. T^* was calculated from the peak of the bulk magnetic susceptibility.

the order of J, so magnetically mediated pairing is possible. For $N_c = 4$ and $\delta = 0.05$, the d-wave pair-field susceptibility diverges at $T_c \approx 0.021$, with an exponent which is less than one, indicating that the fluctuations beyond DMFA which suppress the antiferromagnetism are also responsible for pairing.

The phase diagram of the system is shown in fig. 5. We are determining the phase boundaries by the instability of the paramagnetic phase (divergence of the corresponding susceptibility). Therefore, the overlap of d-wave superconducting and antiferromagnetic phase for dopings $\delta < 0.05$ does *not* indicate a coexistence of these phases. It merely states that if the phase with higher transition temperature is suppressed (*e.g.*, due to impurity effects or long-range interactions not included here) a phase transition at the lower transition temperature might happen from the paramagnetic state.

We also include T^*, the pseudogap temperature fixed by the peak bulk susceptibility. At low temperatures, it serves as a boundary separating the observed Fermi-liquid and non-Fermi-liquid behavior. For $T < T^*$ and $\delta < 0.2$ the self-energy shows non-Fermi-liquid character for the parts of the Fermi surface closest to $\boldsymbol{k} = (\pi, 0)$ whereas the low-temperature self-energy is Fermi-liquid–like for $\delta \gtrsim 0.2$. The d-wave transition temperature is maximum at $\delta \approx 0.05$. The superconductivity persists to large doping, with T_c dropping very slowly. In contrast to experimental findings, the pairing instability (preceded by an AF instability) persists down to very low doping. One possible reason for this is that the model remains very compressible down to very low doping $\delta \sim 0.025$. This could be due to the lack of long-ranged dynamical spin correlations or stripe formation which could become more relevant as N_c increases or when multiple Hubbard planes are coupled together. The effect of such additional non-local corrections ($N_c > 4$) is presently unknown. However, we believe that a finite mean-field coupling between Hubbard planes will stabilize the character of the phase diagram presented here as N_c increases. A finite interplane coupling will also invalidate the Mermin-Wagner theorem, preventing a vanishing T_N for the AF phase as N_c increases. Such work is currently in progress.

Conclusion. – We have used QMC and DCA to study the effect of the initial non-local corrections on the phase diagram of the 2D Hubbard model at intermediate coupling $U = W$. The corrections make significant changes, including a strong suppression of the antiferromagnetism, the emergence of non-Fermi-liquid (pseudogap) and d-wave superconducting regimes. The critical exponent of the pair-field susceptibility is smaller than one, whereas the antiferromagnetic susceptibility diverges with a critical exponent larger than one. This indicates that the same fluctuations that suppress antiferromagnetism upon doping mediate pairing. At half-filling the formation of the Mott gap of width $\gg J$ suppresses pairing.

* * *

It is a pleasure to acknowledge useful discussions with P. G. J. VAN DONGEN, B. GYORFFY, D. HESS, C. HUSCROFT, J. KELLER, H. R. KRISHNAMURTHY, S. MOUKOURI, TH. PRUSCHKE and J. ZAANEN. This work was supported by NSF grants DMR-0073308 and PHY94-07194. Computer support was provided by the Ohio Supercomputer Center.

REFERENCES

[1] For a reviews, see MAPLE M. B., *J. Magn. & Magn. Mater.*, **177-181** (1998) 18; TALLON J. L. and LORAM J. W., to be published in *Physica C* (cond-mat/0005063).
[2] ANDERSON P. W., *The Theory of Superconductivity in the High-T_c Cuprates* (Princeton University Press, Princeton) 1997.
[3] For a review, see SCALAPINO D. J., cond-mat/9908287.
[4] MONTHOUX P. *et al.*, *Phys. Rev. Lett.*, **67** (1991) 3448.
[5] TIMUSK T. and STATT B., *Rep. Prog. Phys.*, **62** (1999) 61.
[6] ZHA Y. *et al.*, *Phys. Rev. B*, **54** (1996) 7561.
[7] HETTLER M. H. *et al.*, *Phys. Rev. B*, **58** (1998) 7475; HETTLER M. H. *et al.*, *Phys. Rev. B*, **61** (2000) 12739.
[8] MAIER TH. *et al.*, *Eur. Phys. J. B*, **13** (2000) 613; MAIER TH. *et al.*, *Phys. Rev. Lett.*, **85** (2000) 1524.
[9] HUSCROFT C. *et al.*, *Phys. Rev. Lett.*, **86** (2001) 139.
[10] LICHTENSTEIN A. I. and KATSNELSON M. I., cond-mat/9911320. These authors use the DCA to study the superconductivity of the Hubbard model; however, they interpolate the self-energy while iterating the DCA equations, which may violate causality.
[11] MOUKOURI S. *et al.*, to be published in *Computer Simulations in Condensed Matter Physics VII*, edited by LANDAU D. P., MON K. K. and SCHUTTLER H. B. (Springer-Verlag, Heidelberg, Berlin).
[12] HIRSCH J. E. and FYE R. M., *Phys. Rev. Lett.*, **56** (1986) 2521.
[13] JARRELL M. and GUBERNATIS J. E., *Phys. Rep.*, **269** (1996) 135.
[14] PRUSCHKE T. *et al.*, *Adv. Phys.*, **42** (1995) 187; GEORGES A. *et al.*, *Rev. Mod. Phys.*, **68** (1996) 13.
[15] MOUKOURI S. *et al.*, unpublished.
[16] JARRELL M., *Phys. Rev. Lett.*, **69** (1992) 168; JARRELL M. and PRUSCHKE TH., *Z. Phys. B*, **90** (1993) 187.